Maximum-Exponent Scaling Behavior of Optical Second-Harmonic Generation in Finite Multilayer Photonic Crystals

Marco Liscidini,[1] Andrea Locatelli,[2] Lucio Claudio Andreani,[1] and Costantino De Angelis[2]

[1]*Dipartimento di Fisica "A. Volta", Università degli Studi di Pavia, via Bassi 6, 27100 Pavia, Italy*
[2]*Dipartimento di Elettronica per l'Automazione, Università degli Studi di Brescia, via Branze 38, 25123 Brescia, Italy*
(Received 21 December 2006; published 3 August 2007)

Scaling laws of second-harmonic generation (SHG) in nonlinear Bragg stacks (or finite one-dimensional photonic crystals) as a function of the number N of periods are explored. While it is known that SHG scales like the sixth power of N when phase matching is achieved, we find maximal scaling like the eighth power of N under appropriate non-phase-matching conditions with the pump and harmonic waves being resonant with band-edge states. In this framework we introduce the concept of self-adaptive coherence length that scales with the system length. An analytical treatment based on coupled-mode equations clarifies the conditions for obtaining different scaling laws as a function of filling factor in the photonic gap map.

Periodic structures have been studied for a long time as a means to achieve high efficiency for second-harmonic generation (SHG) in nonlinear media. The concept of quasiphase matching has proven to be a very useful one in order to enhance nonlinear conversion [1,2]. Recently, there has been much interest for resonant SHG in Bragg multilayers, which can also be viewed as finite one-dimensional (1D) photonic crystals [3–17]. Strong enhancement of SHG takes place when the pump and/or harmonic waves are resonant with band-edge states that are formed in the finite structure. In particular, phase matching occurs when the pump beam is tuned to the first band-edge resonance of the mth order stop band and the harmonic beam is tuned to the second resonance of the $2m$th order stop band [4]. Under these conditions, SHG efficiency has been shown to scale like N^6, where N is the number of periods [5]. Experimentally, scaling faster than N^5 has been demonstrated in $Al_xGa_{1-x}As$/Alox (oxidized AlAs) multilayers [6].

It was recently argued that N^8 scaling for SHG can be realized by combining field enhancement at the pump frequency (contributing like N^4), field enhancement at the second harmonic (contributing like N^2) and phase matching (yielding an additional N^2 increase) [7]. Also, numerical evidence for N^8 scaling in a more complex structure with four-layer unit cell under phase-matching conditions had been claimed [8]. However, these conclusions are in contrast with theoretical and experimental evidence [5,6] that phase-matched SHG in finite Bragg multilayers scales no faster than N^6. Recently, use of non-phase-matched structures to increase nonlinear conversion efficiency with respect to phase-matched ones has been considered in Ref. [9], where 1 order of magnitude increased efficiency was found numerically for a particular multilayer structure, but the scaling law for SHG was not analyzed. Altogether, the issue of SHG scaling in 1D photonic structures is still not clarified.

In this Letter we show that N^8 scaling of SHG efficiency can be achieved in properly designed Bragg multilayers with a simple two-layer unit cell. This maximal scaling takes place when the pump and harmonic waves are both tuned to the first band-edge resonances at the second-to-fourth stop-band edges, in a situation when phase-matching conditions are not fulfilled. A key tool for the analysis is the photonic gap map of the 1D photonic crystal, which allows us to distinguish separate regions as a function of filling factor in which N^8 or N^4 scaling occurs for non-phase-matched SHG. An analytical model based on coupled-mode equations clarifies the conditions which lead to different scaling behavior. The results are consistent with those of the numerical treatment and yield a complete picture of the scaling laws of SHG in connection with band-edge resonances.

Figure 1(a) shows a particular example of the general class of Bragg grating structures we are considering in this Letter. We choose to work with $Al_{0.25}Ga_{0.75}As$/Alox multilayers and use frequency-dispersive optical constants [10]. Figure 1(b) displays the calculated transmittance for a non-$\lambda/4$ structure with $N = 10$ periods. The opening of stop bands up to 4th order can be recognized. Solid arrows indicate the first band-edge resonances at the 2nd order and 4th order stop bands, while the dotted arrow marks the second resonance at the 4th order stop band. Phase matching is verified only when the harmonic wave is tuned to the second resonance [4]. Here we consider SHG with the pump and harmonic waves being resonant with the first band-edge states of the 2nd and 4th order stop bands, respectively.

It is useful to exploit the concept of photonic gap maps for the 1D structures under study. The gap maps for $Al_{0.25}Ga_{0.75}As$/Alox multilayers up to 4th order are shown in Fig. 2 (inset). The main panel represents the 2nd and 4th order stop bands in terms of the pump frequency, in order to visualize the overlapping of band edges which
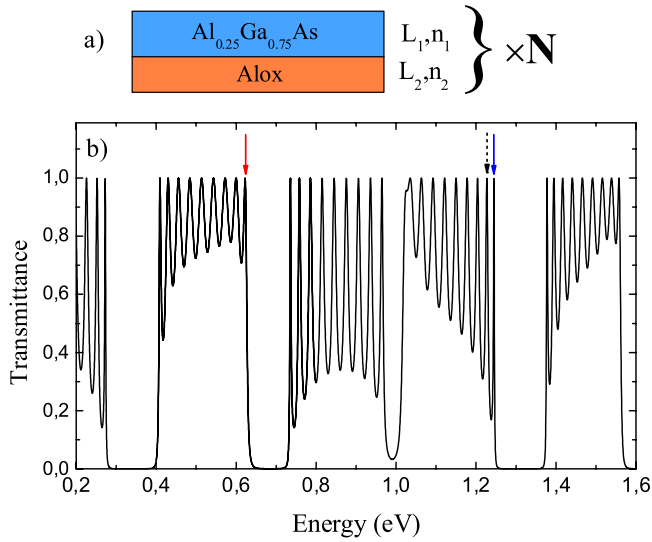
FIG. 1 (color online).   (a) Schematic of a two-layer unit cell for a Bragg multilayer with N periods; (b) linear transmittance for a $Al_{0.25}Ga_{0.75}As$/Alox multilayer with $L_1 = L_2 = 373$ nm and $N = 10$ periods.

may give rise to doubly resonant SHG. The 2nd order gap has two lobes, while the 4th order gap has four lobes which identify four different regions named I, II, III, IV in Fig. 2. The arrows indicate working points for band-edge resonances.

We calculate SHG by the multilayers by means of the nonlinear transfer-matrix method [11]. The $Al_{0.25}Ga_{0.75}As$/Alox stacks are assumed to be oriented along a [111] direction, so that we can restrict the calculation to normal incidence and still have a finite nonlinear polarization by the $\chi^{(2)}$ susceptibility tensor. In real samples, it will be convenient to work at oblique incidence
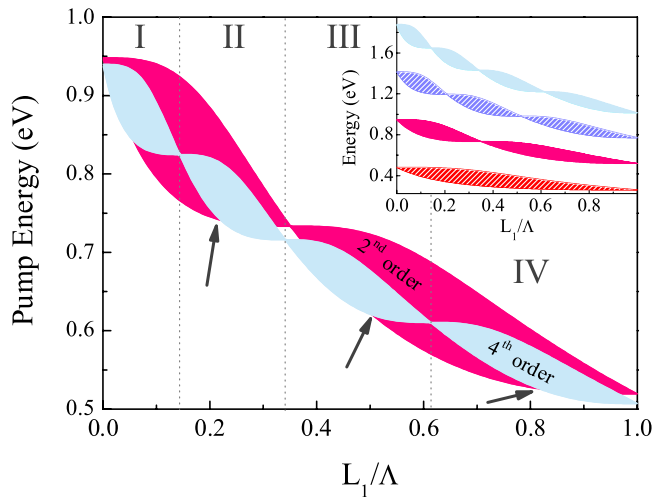
and to use the angle as a tuning parameter. We calculate the scaling of SHG in transmission as a function of N, assuming a pump energy of 0.62 eV (corresponding to $\lambda = 2$ μm wavelength) for the first band-edge resonances marked by solid arrows in Fig. 1(b). For the intersection points shown in Fig. 2, the period Λ has to be modified in order to work with a fixed pump wavelength. In Fig. 3 we show the scaling behavior corresponding to regions II, III, and IV. Scaling like N^8 occurs for double resonance in region III: this result is a most surprising one, since maximal scaling is found in a non-phase-matched situation. On the other hand, scaling like N^4 is observed for double resonance in regions II and IV.

By following the effective-index approach of Ref. [4], in the case of doubly resonant conditions at the mth and $2m$th order gaps, we obtain the effective wave vectors

$$k_\omega = \frac{\pi}{L}(mN - 1), \qquad k_{2\omega} = \frac{\pi}{L}(2mN - 1), \quad (1)$$

with a thickness $L = N\Lambda$. This gives a coherence length

$$L_{\text{coh}} = \frac{\pi}{|k_{2\omega} - 2k_\omega|} = L = N\Lambda. \quad (2)$$

Since in this situation the coherence length of the nonlinear process scales with the number of periods and is always equal to the physical length of the device, the system is characterized by what we call a self-adaptive coherence length. It is worth noting that this is a peculiar regime of SHG scaling in periodic structures that has never been exploited before. We can get the condition of self-adaptive coherence length also at the first-to-second stop-band edges. Nevertheless the analysis of that case is not pursued here, since we have verified that the region of the gap map characterized by N^8 scaling law is not easily accessible with realistic optical and geometric parameters.

FIG. 2 (color online).   Gap maps of $Al_{0.25}Ga_{0.75}As$/Alox multilayers with $\Lambda = 747$ nm period. The main panel displays the 2nd order stop band (pump) and the 4th order stop band (harmonic) as a function of pump frequency, while the inset shows the first four stop bands.
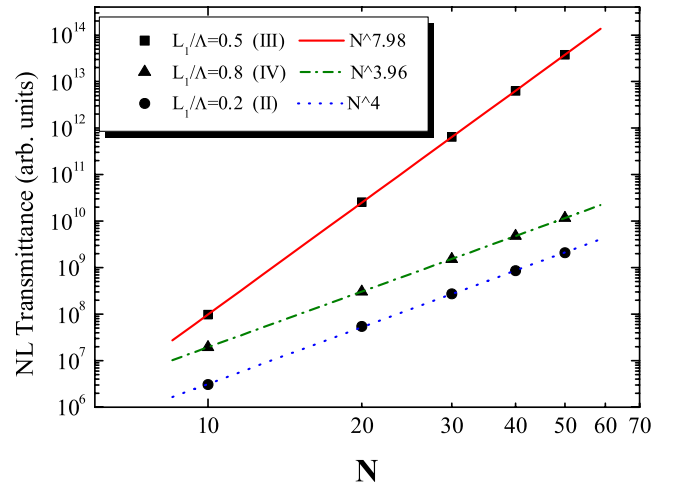
FIG. 3 (color online).   Nonlinear transmittance as a function of number of periods, for $Al_{0.25}Ga_{0.75}As$/Alox multilayers with three different filling factors in regions II, III and IV of Fig. 2. The period Λ has been chosen in order to achieve double resonance at a pump frequency 0.62 eV. The interpolating lines give the fits with power laws.

Still, we have to understand the role of field enhancement in determining different scaling laws in different regions of the gap map. To this goal we derive a simple coupled-mode theory that clarifies the behavior of SHG scaling with length. It is worth noting that the reported model constitutes an extension of the treatment described in Ref. [5], where attention was focused on phase-matched SHG with pump and second-harmonic fields tuned near the first and the second-order stop band, respectively. Here we remove the assumptions on the stop band and resonance orders and demonstrate that a simple plane-wave model can capture all the peculiar features of second-order non-linear interactions we have observed.

We are analyzing the behavior of one-dimensional periodic structures, then it is useful to express the optical parameters in terms of their Fourier expansion

$$n^2(z, \omega) = n_0^2(\omega) + \sum_{m \neq 0} \delta_m \exp(jmPz),$$

$$n_{10}^2 = n_0^2(\omega_0), \qquad n_{20}^2 = n_0^2(2\omega_0), \qquad (3)$$

$$\chi^{(2)}(z) = \frac{n_{20}\lambda}{2\pi} \left[d_0 + \sum_{m \neq 0} d_m \exp(jmPz) \right],$$

where $n(z, \omega)$ is the refractive index profile, $\chi^{(2)}(z)$ is the second-order nonlinear susceptibility profile and $P = 2\pi/\Lambda$, with Λ the grating period. To first order we may assume that dispersion affects only the average components of the linear refractive index (n_{10}, n_{20}).

First we solve the problem at the pump frequency in the undepleted pump approximation. We want to calculate the solutions for the forward (E_{1f}) and the backward (E_{1b}) fields by neglecting linear loss and nonlinear coupling; thus, we define $k_1 = (2\pi/\lambda)n_{10}$ and write

$$E_1(z) = E_{1f}(z) \exp(-jk_1z) + E_{1b}(z) \exp(jk_1z). \qquad (4)$$

We insert this ansatz into the Helmholtz equation and solve the resulting coupled equations to get the slowly varying components of the field. If we assume to work on the generic N_1th band-edge resonance near the mth order stop band, and impose the proper boundary conditions ($E_{1f}(0) = E_0$ and $E_{1b}(L) = 0$), we have

$$E_{1f}(z) = E_0 \left[\cos(\Phi_1 z) - j \frac{\Delta_1 L}{2N_1\pi} \sin(\Phi_1 z) \right] \exp[j(\Delta_1/2)z]$$

$$= \alpha E_0 \exp[j(\Delta_1/2)z],$$

$$E_{1b}(z) = jE_0 \frac{C_1 L}{N_1\pi} \sin(\Phi_1 z) \exp[-j(\Delta_1/2)z]$$

$$= \beta E_0 \exp[-j(\Delta_1/2)z], \qquad (5)$$

where $\Delta_1 = 2k_1 - mP$ is a detuning parameter, $C_1 = (\pi\delta_m)/(\lambda n_{10})$ is the coupling coefficient (we assume real δ_m), and the dominant wave number Φ_1 reads as

$$\Phi_1 = \sqrt{\left(\frac{\Delta_1}{2}\right)^2 - C_1^2} = \frac{N_1\pi}{L}. \qquad (6)$$

At the second-harmonic we decompose the field $E_2(z)$ into a forward (E_{2f}) and backward component (E_{2b}), as done in Eq. (4) for the pump field, with $k_2 = (4\pi/\lambda)n_{20}$. We calculate the nonlinear forcing terms by taking the square of the pump field, multiplied by the Fourier-expanded nonlinear susceptibility $\chi^{(2)}(z)$, and we retain only the fast-varying terms that oscillate with similar wave number. This condition forces us to work near the $2m$th order stop band, where we tune the second-harmonic field to the generic N_2th band-edge resonance. With these assumptions we evaluate the dominant wave number Φ_2 at the second harmonic

$$\Phi_2 = \sqrt{\left(\frac{\Delta_2}{2}\right)^2 - C_2^2} = \frac{N_2\pi}{L}, \qquad (7)$$

where $\Delta_2 = 2(k_2 - mP)$ and $C_2 = 2(\pi\delta_{2m})/(\lambda n_{20})$. We then write $E_{2f} = \exp[j(\Delta_2/2)z]F(z)$ and $E_{2b} = \exp[-j(\Delta_2/2)z]B(z)$ and we get the governing equations for F and B

$$jF_z - \frac{\Delta_2}{2}F = C_2B + E_0^2(d_0\alpha^2 + 2d_m\alpha\beta),$$
$$\qquad\qquad\qquad\qquad\qquad\qquad\qquad\qquad (8)$$
$$-jB_z - \frac{\Delta_2}{2}B = C_2F + E_0^2(d_0\beta^2 + 2d_m\alpha\beta).$$

The system of coupled Eqs. (8) governs the evolution of $F(z)$ and $B(z)$ when the pump and second-harmonic fields are tuned to generic band-edge resonances near the mth and the $2m$th order stop band, respectively. However, we are interested in the specific case of self-adaptive coherence length with pump and second-harmonic fields tuned to the first band-edge resonances near the 2nd and the 4th order stop band. Thus we fix $N_1 = N_2 = 1$, we take $m = 2$ and solve the system to find the modulus of the second-harmonic field at the output

$$|F(L)| = \frac{E_0^2 L^2}{6\pi^4} \{ -L^2[(8C_1^2 C_2 - \Delta_1^2 \Delta_2)d_0$$
$$\qquad - 4C_1\Delta_1(2C_2 - \Delta_2)d_m]$$
$$\qquad + 2\pi^2[(2\Delta_1 - \Delta_2)d_0 - 4C_1 d_m] \}. \qquad (9)$$

Nonlinear conversion efficiency is proportional to $|F(L)|^2$. Further approximation is needed in order to highlight the scaling behavior of SHG. We introduce two new parameters $e_i = \Delta_i L/(2\pi)$, with $i = 1, 2$ for the pump and the second harmonic, respectively. These terms are related to the enhancement of the field intensity due to the resonant periodic structure; thus, in the strong grating approximation we have $|e_i| \gg 1$. We introduce this ansatz into Eqs. (6) and (7) and the resulting expressions for C_i are simplified through a truncated Taylor expansion

$$C_i \simeq \frac{\pi}{L}\left(e_i - \frac{1}{2e_i}\right)\text{sgn}(\Delta_i C_i). \qquad (10)$$

Now we can rewrite Eq. (9) as a function of e_1 and e_2:

$$|F(L)| = AL\left\{ \left[2e_1^2 e_2(1-s_2) + \frac{e_1^2}{e_2}s_2 \right](d_0 - 2d_2 s_1) \right.$$
$$+ 2e_1(d_0 - d_2 s_1) + e_2[d_0(-1 + 2s_2)$$
$$\left. + 2d_2(1-s_2)s_1] \right\}, \tag{11}$$

with $A = 2E_0^2/(3\pi)$, $s_1 = \text{sgn}(\Delta_1 C_1)$, and $s_2 = \text{sgn}(\Delta_2 C_2)$. If we note that each factor e_i incorporates a linear dependence on L, it is straightforward to conclude that the sign of the product between detuning Δ_2 and coupling coefficient C_2 at the second harmonic is critical to determine the scaling with length of the conversion efficiency. In particular, when $\text{sgn}(\Delta_2 C_2) = -1$ we have

$$|F(L)| \simeq 4ALe_1^2 e_2(d_0 - 2d_2 s_1), \tag{12}$$

and we can observe an L^8 scaling of the second-harmonic intensity. Notice that, as opposed to the phase-matched case where field enhancement at pump and second-harmonic frequencies contributes only to an L^4 scaling of the second-harmonic intensity ($|F(L)| \propto e_n e_m$, n, $m = 1$, 2) [5], in the self-adaptive coherence length regime field enhancement can contribute up to an L^6 scaling ($|F(L)| \propto e_1^2 e_2$ in Eq. (12)). Conversely, when $\text{sgn}(\Delta_2 C_2) = 1$ we get

$$|F(L)| \simeq AL\left[\frac{e_1^2}{e_2}(d_0 - 2d_2 s_1) + d_0 e_2 + 2e_1(d_0 - d_2 s_1) \right] \tag{13}$$

and the second-harmonic intensity scales as L^4. This confirms that the self-adaptive coherence length regime by itself is not a sufficient condition to get maximal scaling, as field interference has to be properly optimized.

The analytical treatment demonstrates that it is possible to switch between two scaling regimes ($\propto L^8$ and $\propto L^4$, respectively), in agreement with the numerical simulations reported in the first part of the Letter. Moreover, the SHG scaling with length is determined by the sign of the product between Δ_2 and C_2. We always choose a negative sign of detuning parameters Δ_i since this choice permits to tune the fields to low-frequency band-edge resonances, where the optical energy is mostly confined into the high-index regions. In the cases of interest we analyze the behavior of the sign of C_2. The expression for the Fourier coefficients δ_{2m} of a square grating reads as

$$\delta_{2m} = \frac{1}{2m\pi}(n_1^2 - n_2^2)\sin\left(2m\pi\frac{L_1}{\Lambda}\right), \tag{14}$$

where L_1 is the thickness of the high-index layers, and $m = 2$ when we deal with the case of second-harmonic field tuned near the 4th order stop band. As we vary L_1 between 0 and Λ we find four different working regions: (i) $0 < L_1/\Lambda < 0.25$: δ_4 and then C_2 are positive, the conversion efficiency is proportional to L^8; (ii) $0.25 < L_1/\Lambda < 0.5$: δ_4 and then C_2 are negative, the conversion efficiency is proportional to L^4; (iii) $0.5 < L_1/\Lambda < 0.75$: δ_4 and then C_2 are positive, the conversion efficiency is

proportional to L^8; (iv) $0.75 < L_1/\Lambda < 1$: δ_4 and then C_2 are negative, the conversion efficiency is proportional to L^4. When the coupling coefficient C_2 is zero we have a vanishing stop band at the second harmonic. This condition corresponds to the transitions between 4th order lobes with different SHG scaling in the gap maps of Fig. 2. Although coupled-mode theory fails to give quantitatively the filling factors at lobe boundaries and the stop-band widths in the case of strong gratings, the alternation between lobes with N^4 or N^8 scaling is in perfect agreement with the results of the numerical simulations. Furthermore, it has been demonstrated [5] that this analytical procedure is able to estimate the second-harmonic intensity (and then the scaling with length) also in the critical case of high-index-contrast gratings.

In conclusion, SHG efficiency in a Bragg multilayer can scale as N^8 in a non-phase-matched regime when pump and harmonic waves are tuned to the band-edge resonances at the 2nd and 4th order stop band, respectively. This optimum scaling is due to maximal combination of field enhancement at the pump and harmonic frequencies in a condition of self-adaptive coherence length, which is always equal to the physical length of the system. By varying the filling factor, alternation between N^8 and N^4 scaling is demonstrated both numerically and analytically, corresponding to different lobes in the 1D photonic gap map. The results challenge the commonly held view that phase matching has to be fulfilled for optimum scaling, and may also prove important for nonlinear interactions in photonic crystals of higher dimensionality.

[1] N. Bloembergen and A. J. Sievers, Appl. Phys. Lett. **17**, 483 (1970).
[2] J. P. van der Ziel and M. Ilegems, Appl. Phys. Lett. **29**, 200 (1976).
[3] M. Scalora *et al.*, Phys. Rev. A **56**, 3166 (1997).
[4] M. Centini *et al.*, Phys. Rev. E **60**, 4891 (1999).
[5] C. De Angelis *et al.*, J. Opt. Soc. Am. B **18**, 348 (2001).
[6] Y. Dumeige *et al.*, Phys. Rev. Lett. **89**, 043901 (2002).
[7] T. Ochiai and K. Sakoda, Opt. Express **13**, 9094 (2005).
[8] G. T. Kiehne, A. E. Kryukov, and J. B. Ketterson, Appl. Phys. Lett. **75**, 1676 (1999).
[9] M. Centini *et al.*, Opt. Lett. **29**, 1924 (2004).
[10] *Handbook of Optical Constants of Solids*, edited by E. D. Palik (Academic, Orlando, FL, 1991).
[11] D. S. Bethune, J. Opt. Soc. Am. B **6**, 910 (1989).
[12] Y. Dumeige *et al.*, Appl. Phys. Lett. **78**, 3021 (2001).
[13] G. D'Aguanno *et al.*, Opt. Lett. **24**, 1663 (1999).
[14] G. D'Aguanno *et al.*, Phys. Rev. E **64**, 016609 (2001).
[15] M. Liscidini and L. C. Andreani, Appl. Phys. Lett. **85**, 1883 (2004).
[16] M. Liscidini and L. C. Andreani, Phys. Rev. E **73**, 016613 (2006).
[17] X. Vidal and J. Martorell, Phys. Rev. Lett. **97**, 013902 (2006).